Earthquake sequence of 1938-1939 in Mogollon Mountains, New Mexico

James Taggart and Frank Baldwin

New Mexico Geology, v. 4, n. 4 pp. 49-52, Print ISSN: 0196-948X, Online ISSN: 2837-6420.
https://doi.org/10.58799/NMG-v4n4.49

This page is intentionally left blank to maintain order of facing pages.

New Mexico GEOLOGY
• Science and Service
Volume 4, No. 4, November 1982

Earthquake sequence of 1938–1939 in Mogollon Mountains, New Mexico

by *James Taggart* and *Frank Baldwin*, U.S. Geological Survey, Denver, CO 80225

Abstract

Earthquake reports and observational data from seismographs at Tucson Magnetic Observatory (TUO) are used to describe 100 of nearly 400 recorded earthquakes that occurred in the Mogollon Mountains, southwestern New Mexico, between 5 September 1938 and 31 October 1939. $S_g - P_g$ interval times are used with regional crustal-velocity models to estimate epicentral distances from TUO. The nominal epicenters of the earthquakes are at 33.3° N., 108.5° W., with a radius of uncertainty of approximately 20 km. Reports of residents and observers suggest that a few of the larger earthquakes had maximum Modified Mercalli (MM) intensities of VI. The falloff of MM intensity isoseisms around the largest earthquake (17 September 1938, 17 20 17 UTC) yields an estimate of $m_{b,int} = 4.9$. This event contributed about 30% of the total seismic energy of the sequence. L_g amplitudes are used to estimate the relative magnitudes of the other earthquakes with respect to the 17 September 1938 earthquake. Among known New Mexico earthquakes, the total seismic energy of the Mogollon Mountains sequence is second only to that of the 1906–1907 sequence near Socorro.

Introduction

During the course of checking lists of New Mexico events for inclusion in a national earthquake catalog, we noted discrepancies and data without references among a sequence of earthquakes that occurred in 1938 and 1939. Intensity reports for a few of these earthquakes suggest that the epicenters were in the Mogollon Mountains of southwestern New Mexico, slightly more than 2° from the Tucson Magnetic Observatory (TUO). We decided to check the TUO seismograms to resolve the discrepancies and to identify as many events as possible in the sequence.

The uncalibrated seismic instrumentation at TUO in 1938 and 1939 consisted of vertical short-period and broadband Benioff seismographs and two horizontal Wood–Anderson seismographs. The two horizontal and two vertical optically coupled signals were recorded on drum-mounted photographic paper at resolutions of 60 mm/min for the short-period vertical component and 30 mm/min for the other components. Arrival times, trace amplitudes, and periods of several phases for each earthquake were measured on a scanning viewer at two-thirds original scale from 35-mm negative copies of the seismograms. Daily clock errors did not exceed 0.5 second and the clock adjustments are clearly marked on the seismograms. We estimate that the measured times are accurate to ±0.5 second on the short-period vertical seismograms and ±1.0 second on the other components.

Location

The Mogollon Mountains comprise a broad, deeply dissected area of Oligocene and Miocene volcanic rocks of caldera origin. The volcanic terrane has been modified and complicated by the development of basin-and-range structure in late Tertiary time (Ratté and others, 1979). The general location of the range, north and east of Buckhorn, New Mexico, is shown in fig. 1. Earthquake reports (U.S. Coast and Geodetic Survey, 1938, 1939) identify nearly thirty earthquakes that probably occurred in this area during the period from 17 September 1938 through 29 July 1939. Several hundred additional unidentified earthquakes were felt in the area during this period. Summaries of the reports are given by Neumann (1940) for eight of the earthquakes in 1938, and by Bodle (1941) for 13 of the earthquakes in 1939.

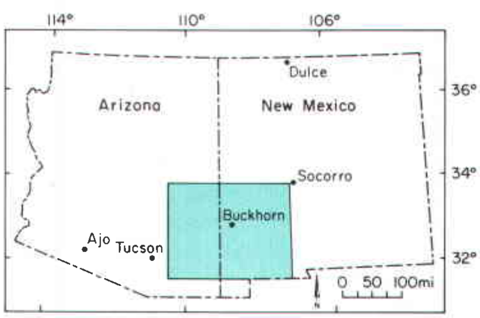

FIGURE 1—MOGOLLON MOUNTAINS OF SOUTHWEST NEW MEXICO LOCATED A FEW KILOMETERS NORTH AND EAST OF BUCKHORN; area of fig. 2 shown by shaded area.

The largest and most completely described of these earthquakes occurred on 17 September 1938 at about 1720 UTC (Universal Time, Coordinated). Neumann (1940, fig. 6) estimated the maximum intensity and the extent of the area in which this earthquake was felt. We reviewed the reports for the earthquake (U.S. Coast and Geodetic Survey, 1938) and assigned Modified Mercalli (MM) intensities to various reporting localities. Fig. 2 shows an isoseismal map interpreted from the distribution of intensities. Three other large earthquakes in the sequence exhibit similar, but less complete, distributions of intensities. The smaller earthquakes in the sequence were felt at localities near or within the larger intensity (VI) isoseism in fig. 2.

The measured $S_g - P_g$ differential arrival times at TUO from identified earthquakes in the sequence fall between 28.5 and 30.5 seconds. Seismograms from 01 July 1938 through 31 October 1939 were checked for events with $S_g - P_g$ in this range. These events are easily identified on the seismograms because there are no observed $S_g - P_g$ times of 24.5 to 28.5 seconds or 30.5 to 34.0 seconds. The first earthquake in the sequence occurred on 05 September 1938 and small events continued to occur sporadically through October 1939. Arrival times at TUO of the P_n, P_g, and S_g phases from approximately 150 earthquakes of the sequence were measured on as many of the four components as possible. P_g arrival times were noted to the nearest minute and $S_g - P_g$ time intervals to the nearest second for nearly 250 additional small earthquakes. Many smaller events probably were undetected in the background noise of the short-period vertical seismograms, but few if any measurable events were lost during the daily recorded changes, which generally required less than two minutes.

Intensity constraints (see fig. 2) suggest that the epicenters could not be much farther from TUO than the White Creek Ranger Station nor closer to TUO than the town of Buckhorn. This sets an upper limit of approximately 260 km and a lower limit of approximately 225 km on the epicentral distances from TUO. In order to estimate epicentral distance from $S_g - P_g$ time intervals, we assume that the earthquakes occurred within the upper layer of the crust and that the identification of the P_g and S_g phases is correct.

The difference in the travel times of the P_g and S_g phases is represented by

$$t_{S_g} - t_{P_g} = \Delta/V_S - \Delta/V_P + c_2 - c_1 \qquad (1)$$

where Δ is epicentral distance in km, V_P and ☞

ALSO IN THIS ISSUE:

COMING SOON

Historical vignette—Stephenson-Bennett mine
Geology and coal resources of Alamo Band Navajo Reservation

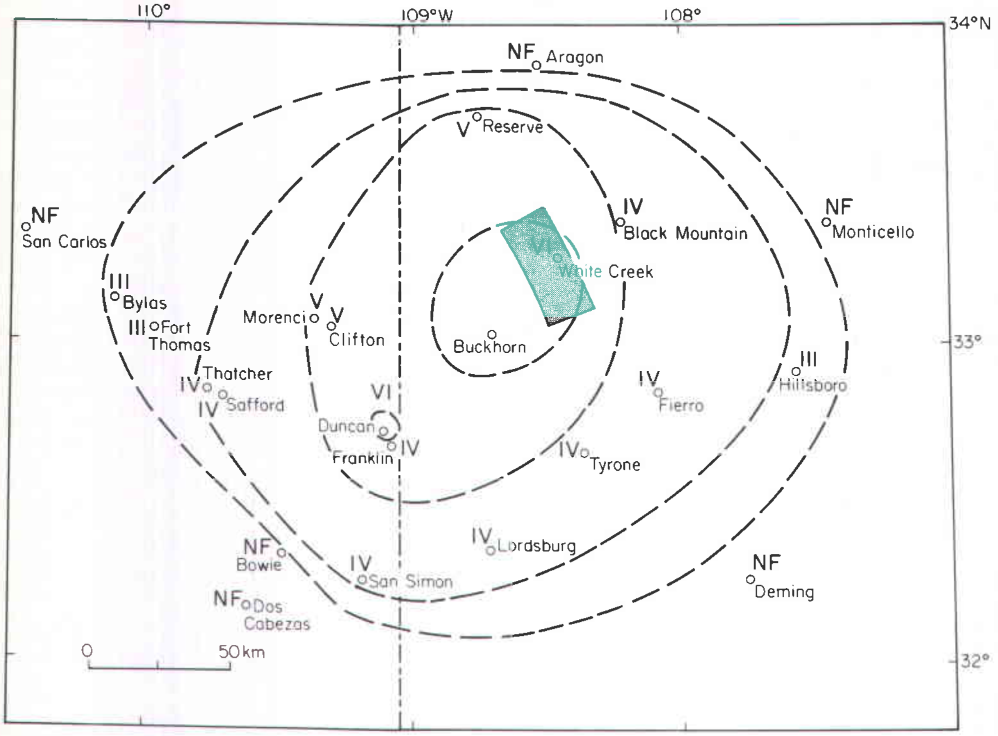

FIGURE 2—ISOSEISMAL MAP FOR LARGEST MOGOLLON MOUNTAINS EARTHQUAKE ON 17 SEPTEMBER 1938 AT 1720 UTC; epicentral region of earthquakes, based on data from TUO, shown by shaded area.

V_S are the P_g and S_g velocities in km/second, and c_1 and c_2 are the P_g and S_g intercepts, respectively, in seconds. Equation (1) can be used to determine a range of reasonable velocity models where either V_P or Poisson's ratio is allowed to vary. c_1 and c_2 are set arbitrarily at 1.0 and 2.0 seconds for explosion paths and at 0.5 and 1.0 seconds for earthquake paths. Gish and others (1981) estimate P_g velocities ranging from 5.84 to 6.11 km/second along a profile between Globe, Arizona, and Tyrone, New Mexico, but they do not report S_g velocities. Warren (1969) suggests that Poisson's ratio is about 0.22 in the Colorado Plateau region. Testing these values against explosion data from the Basin and Range province of southern Arizona is appropriate.

Two large blasts (35,350 and 44,000 lbs of explosives) at the Ajo, Arizona, open-pit porphyry-copper mine are identified on the TUO short-period vertical seismograms for 31 May and 05 June 1939. The presumed P_g and S_g crustal phases are sharply defined with $S_g - P_g$ intervals of 23.0 and 23.6 seconds. The distance between TUO and the Ajo pit is 191.8 $\pm$1.0 km. If Poisson's ratio is fixed at 0.22, these data require that P_g velocity = 5.8 km/second. Previous estimates (Warren, 1969; Sinno and others, 1981; Gish and others, 1981) of P_g velocity in the Arizona Basin and Range province average about 6.0 km/second. By holding P_g velocity at 6.00 km/second, the explosion data yield a reasonable working model with Poisson's ratio = 0.235, S_g velocity = 3.53 km/second, and average velocity of separation of the S_g and P_g waves = 8.57 km/second.

When the working model is applied to observations from the Mogollon Mountains earthquakes, the estimated epicentral distance from TUO is 240 and 257 km for $S_g - P_g$ intervals of 28.5 and 30.5 seconds. The earthquakes probably occurred within this range of distance from TUO. Other acceptable models change the minimum or maximum epicentral distance by only a few kilometers. The epicentral region, bounded by arcs at 240 and 257 km from TUO, is shown by the diagonal-ruled area in fig. 2. The preferred epicenters for the earthquakes are taken as 33.3° N. latitude and 108.5° W. longitude with location uncertainties that probably do not exceed 20 km. The data do not warrant the estimation of the relative locations of the epicenters with respect to one another.

Magnitude

Measurements of the maximum sustained amplitudes and periods of the P_g and L_g phases were made on as many of the TUO seismograms as possible for approximately 100 of the Mogollon Mountains earthquakes. In addition, coda durations were estimated on the short-period seismograms for approximately 380 earthquakes. The codas for 11 large events, including the largest earthquake, were not recorded because the vertical seismographs were inoperative. In addition, the cutoff times for codas of four large events were obscured by the codas of other earthquakes. No earthquakes with $m_{b,int} \geq 2.5$ were overlooked on the horizontal seismograms as a result of these problems. Duration measurements were also made on the Wood–Anderson seismograms for approximately 50 of the largest earthquakes.

The estimation of magnitudes for the earthquakes is difficult because many of the traces vanish where the amplitude exceeds 2 mm. Nevertheless, a sufficient number of peaks and troughs are discernible to estimate the maximum sustained amplitudes to $\pm$50%, which is equivalent to $\pm$0.2 magnitude unit. Where the amplitudes are less than 2.0 mm, the waves are seen to consist of several intermixed frequencies. As a result, using magnitude formulas that include period (T) is not possible. Also M_L magnitude cannot be estimated reliably because the Richter (1935) distance attenuation factor, Log $(-A_0)$, is inappropriate for use with the nonstandard (T_s = 10 seconds) Wood–Anderson seismographs at TUO. Instead a graphical method is used to estimate the $m_{b,int}$ magnitude of the largest earthquake from isoseisms, and relative amplitudes are used to estimate the equivalent $m_{b,int}$ magnitudes for 100 additional earthquakes of the sequence.

Nuttli and others (1979) discuss the methodology for estimating $m_{b,int}$ magnitude from the falloff of MM intensity with distance. If certain assumptions are accepted, the method is applicable to any shallow earthquake for which well-determined isoseisms are available. We use this method to estimate the $m_{b,int}$ magnitude of the 17 September 1938, 1720 UTC, Mogollon Mountains earthquake. Table 1 lists

TABLE 1—INTENSITY FALLOFF VERSUS DISTANCE, MOGOLLON MOUNTAINS EARTHQUAKE OF 17 SEPTEMBER 1938, 17 20 17 UTC.

Isoseism	Enclosed ellipse a semiaxis (km)	Enclosed ellipse b semiaxis (km)	Nuttli and others (1979) equivalent $(A/T)_z$ for 1-Hz L_g (cm/sec)
VI	30	23	0.0056
V	65	50	0.0022
IV	100	80	0.0011

New Mexico GEOLOGY
• Science and Service
Volume 4, No. 4, November 1982

published quarterly by
New Mexico Bureau of Mines and Mineral Resources
a division of New Mexico Institute of Mining & Technology

Subscriptions: Issued quarterly, February, May, August, November; subscription price $5.00/yr.

Editorial matter: Contributions of possible material for consideration in future issues of NMG are welcome. Address inquiries to Marla D. Adkins-Heljeson, editor of *New Mexico Geology*, New Mexico Bureau of Mines & Mineral Resources, Socorro, NM 87801

Circulation: 1,400

Printer: University of New Mexico Printing Plant

the semimajor (a) and semiminor (b) axial dimensions of the largest ellipses enclosed by the MM IV, V, and VI isoseisms (fig. 2) for this earthquake.

The a and b values, connected by horizontal bars, are plotted in fig. 3 as the maximum and minimum distances at which the MM intensities and the equivalent bedrock-particle velocities (Nuttli and others, 1979) were felt. The intensity bars and Airy phase (L_g wave) attenuation curve for the 9 November 1968 reference earthquake in southern Illinois (upper curve) are taken from Nuttli and others (1979). Attenuation curve templates for eight values of anelastic attenuation (γ) between 0.0006/km and 0.025/km were tested to determine the best fit to the data in table 1. The best fit attentuation curve has $\gamma = 0.01$/km and a projected vertical 1-Hz L_g particle velocity, $(A/T)_z = 0.015$ cm/second, at an epicentral distance of 10 km. This value of $(A/T)_z$ is equivalent to an m_b first approximation (μ) = 5.2, where $(A/T)_z = 0.03$ cm/second and m_b = 5.5 for the reference southern Illinois earthquake. Using equation (2) of Nuttli and others (1979), the true estimate of m_{bLg} (or m_b) for the Mogollon Mountains earthquake should be $m_{b,int} = 4.86$, or 4.9 rounded off.

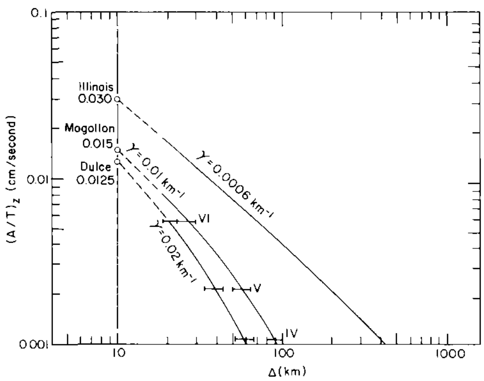

FIGURE 3—ESTIMATION OF APPROXIMATE BODY-WAVE MAGNITUDE, μ, FROM INTENSITY-ATTENUATION DATA; attenuation curve for 1-Hz L_g waves from 9 November 1968, Illinois reference earthquake taken from Nuttli and others (1979). Best-fitting Airy phase dispersion curves and coefficients of anelastic attenuation, γ, are shown for largest Mogollon Mountains earthquakes and for 23 January 1966 Dulce, New Mexico, earthquake; for Illinois, Mogollon Mountains, and Dulce earthquakes, μ = 5.5, 5.2, and 5.12, respectively.

A test of the repeatability of the method yielded $\mu = 5.12$ (fig. 3) and $m_{b,int} = 4.8$ for the 23 January 1966 earthquake at Dulce, New Mexico; whereas Nuttli and others (1979) obtained $m_{b,int} = 4.9$ for this earthquake.

Maximum sustained L_g amplitudes were measured for 48 of the largest earthquakes in the sequence on the TUO Wood–Anderson N–S seismograms. Ignoring the frequency content of the L_g waves and assuming similar focal mechanisms, the estimated magnitude of the other earthquakes is given by

$$m_{b,int} = 4.9 + \log_{10}(A_e/A_{ref}) \quad (2)$$

where A_e and A_{ref} are the trace amplitudes of the other and largest earthquakes. L_g trace amplitudes for 90 earthquakes were measured on the vertical broadband seismograms, including 38 of the 48 large earthquakes measured on the N–S seismograms. Fig. 4 is a plot of the vertical trace amplitudes against magnitudes from equation (2). The cloud of points for these larger earthquakes shows slight curvature that may result from failure to correct for systematic frequency variations in the L_g waves of the earthquakes. In order to estimate the magnitudes of the 52 smaller earthquakes from the vertical trace amplitudes, a curve with slope = 1.0 is fit by inspection to the points rather than fitting by least squares, which would underestimate the magnitudes of the smaller earthquakes. The equation for the inspection-fit curve is

$$m_{b,int} = 2.59 + \log_{10} A_{LZ} \quad (3)$$

where A_{LZ} is the broadband vertical trace amplitude. The magnitudes of 52 earthquakes in the sequence are estimated using equation (3). The maximum scatter of points about the inspection-fit curve is equivalent to approximately ± 0.4 magnitude unit.

Table 2 lists the dates, origin times, $m_{b,int}$ magnitudes from equation (2) or (3), total duration of short-period vertical signals in seconds and MM intensities for 100 of the larger Mogollon Mountains earthquakes. The distribution of magnitudes suggests a swarm-like character for the sequence. A few unidentified earthquakes with $m_{b,int} < 2.5$ on 17–18 September 1938 may have occurred during the time when the vertical seismographs were inoperative.

We investigated whether coda durations observed on the TUO short-period vertical seismograms could be used to estimate the magnitudes of the smaller earthquakes of the sequence. The cut-off time where the coda amplitude has decayed to twice the pre-earthquake background amplitude was measured for approximately 380 earthquakes. The duration for each earthquake is arbitrarily set equal to the cut-off time minus the origin time, $t_c - t_o$. Fig. 5 is a plot of durations against the magnitudes obtained from equations (2) or (3) for 82 of the earthquakes. Again an inspection-fit curve is extended through the points. The maximum scatter of points about this curve is equivalent to approximately ± 0.7 magnitude unit, which suggests that the cascading estimation techniques used here have been carried too far to give reliable magnitudes. Although the smallest identifiable earthquakes have durations of about 90 seconds, W. H. K. Lee (personal communication, 1981) suggests that the technique loses resolution for durations less than 140 seconds (twice the L_g travel time to TUO).

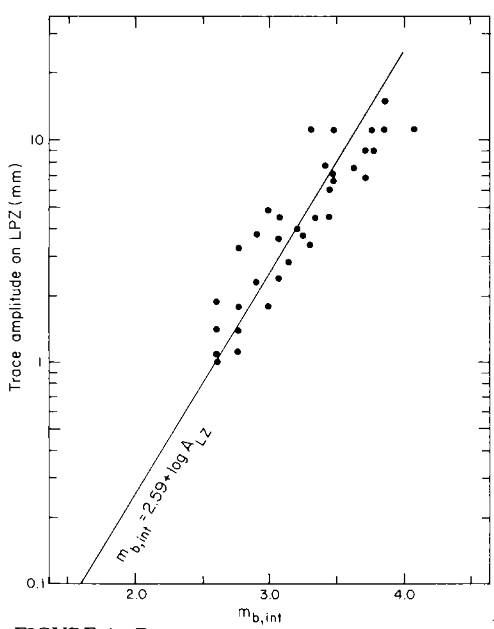

FIGURE 4—PLOT OF MEASURED LONG-PERIOD VERTICAL (LPZ) TRACE AMPLITUDE AGAINST $M_{B,INT}$ FOR MOST OF LARGER EARTHQUAKES IN MOGOLLON MOUNTAINS SEQUENCE; $m_{b,int}$ values are estimated from measured trace amplitudes on TUO N–S Wood–Anderson seismograms using equation (2). Inspection-fit curve, $m_{b,int} = 2.59 + \log A_{LZ}$ with slope = 1.0, is used to estimate $m_{b,int}$ for earthquakes with LPZ trace amplitudes < 2.0 mm.

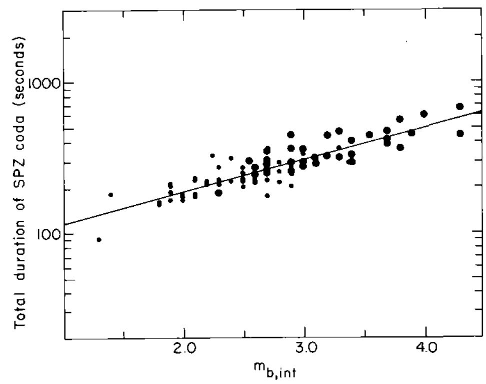

FIGURE 5—PLOT OF $M_{B,INT}$ AGAINST TOTAL SPZ CODA DURATION FOR EARTHQUAKES IN TABLE 2; large and small dots represent estimates of $m_{b,int}$ using equations (2) and (3). Inspection-fit curve could be used to estimate $m_{b,int}$ for additional 300 small earthquakes of Mogollon Mountains sequence, but uncertainty of values would be very large.

Discussion

The $S_g - P_g$ arrival time differences restrict the epicenters within a ring around TUO between radii of 240 and 257 km. Tighter constraint of the epicenters to the vicinity of the White Creek Ranger Station (sec. 1, T. 12 S., R. 16 W.) in the Mogollon Mountains is supported by the fact that 20 identified earthquakes were reported felt in this area, and many of the smaller events are clearly aftershocks of the earthquakes that were felt. Furthermore, no earthquakes or large open-pit mining explosions elsewhere in the above distance range from TUO are known to have occurred in 1938 and 1939.

The arrival time differences of 2.5–4.8 seconds between P_g and P_n waves from the earthquakes suggest as much as 8 km range in focal depths, but the depths cannot be determined in the absence of an accurate velocity model for the P_n path. Intensity reports which seem reliable suggest very shallow depths for a few small earthquakes with $m_{b,int} < 1.0$ that were not discernable on the TUO seismograms.

The magnitude of the largest earthquake in the sequence was estimated using the Nuttli and others (1979) relation for falloff of MM intensity isoseisms versus m_{bLg} magnitude because the observational data from the TUO seismograms were inadequate to permit the direct estimation of magnitudes. The advantages of this method are that it is straightforward and reliable. Independent tests of the method on several earthquakes listed by Nuttli and others (1979) yielded results that agreed within ± 0.20 units of their $m_{b,int}$ values. Our values for γ typically were larger than those of Nuttli and others (1979), but these differences have only a slight effect on the estimate of $m_{b,int}$.

Although the intensity falloff method is reliable, several sources of potential inaccuracy exist in the $m_{b,int}$ values. One uncertainty, mentioned by Nuttli and others (1979), lies in the assignment of single values of vertical ground-motion velocity to the presumed bedrock intensity isoseisms. Also uncertain is the assumption that the largest ellipse contained within an isoseism represents limits to which the intensity was felt on bedrock. In the Western Interior states, the sparse reports seldom represent bedrock intensity observations. Furthermore, the method ignores systematic bias that is directly related to the focal mechanism and radiation pattern of earthquakes.

Ratté and Gaskill (1975) show many normal faults of post-Oligocene age on a reconnaissance map of the Gila Wilderness area, which includes the Mogollon Mountains. Most of the faults trend west-northwest through the area in sets that form complex graben up to 50 km in length. Hot springs occur in some of the graben on the east side of the area. One of the major faults, more than 17 km in length, crosses the West Fork of the Gila River near the White Creek Ranger Station. A less prominent set of faults along the western side of the range trends northeast and may be orthogonal to the principal faults. Surficial faulting was not mentioned in reports of the earthquakes, but rock falls that partially blocked access trails to the ranger station were reported. Evidence is insufficient to confirm that the earthquakes were caused by reactivated dip-slip displacement at depth on either set or both sets of these faults. If this is the case, however, the radiation patterns of the earthquakes would be similar (as observed), and the TUO trace amplitudes would yield reliable estimates of relative magnitudes.

The seismic energy released by the Mogollon Mountains earthquake sequence is of some interest, but only relative values can be estimated accurately. Assuming that log seismic energy is proportional to 1.5 $m_{b,int}$ because the magnitudes are based on L_g amplitudes, we find that 30% of the total seismic energy was released by the 17 September 1938 event and that nearly 300 very small earthquakes not shown in table 2 released energy equivalent to no more than one $m_{b,int} = 3.5$ earthquake. The 17 September 1938 event appears to have been slightly larger than the Dulce, New Mexico, earthquake of 23 January 1966, based on our estimations of $m_{b,int}$. We estimate that the total seismic energy and total seismic moment of the Mogollon Mountains sequence are about three times that of the Dulce sequence (see Herrmann and others, 1980, for an analysis of the main Dulce event). Indeed, the Mogollon Mountains sequence appears to be second only to the 1906–1907 Socorro sequence (see Reid, 1911) in total seismic energy among known New Mexico earthquake sequences.

ACKNOWLEDGMENTS—We appreciate critical reviews of the text by J. W. Dewey and Allan Sanford. Discussions with Carl Stover and W. H. K. Lee helped us evaluate the observational data. Madeleine Zirbes helped format the computer preparation of the tables and text.

References

Bodle, R. R., 1941, United States earthquakes, 1939: U.S. Department of Commerce, Coast and Geodetic Survey, Serial 637, p. 1–69

Gish, D. M., Keller, G. R., and Sbar, M. L., 1981, A refraction study of deep crustal structure in the Basin and Range–Colorado Plateau of eastern Arizona: Journal of Geophysical Research, v. 86, p. 6,029–6,038

Herrmann, R. B., Dewey, J. W., and Park, Sam-Kuen, 1980, The Dulce, New Mexico, earthquake of 23 January 1966: Seismological Society of America, Bull., v. 70, p. 2,171–2,183

Neumann, Frank, 1940, United States earthquakes, 1938: U.S. Department of Commerce, Coast and Geodetic Survey, Serial 629, p. 1–59

Nuttli, O. W., Bollinger, G. A., and Griffiths, D. W., 1979, On the relation between Modified Mercalli intensity and body-wave magnitude: Seismological Society of America, Bull., v. 69, p. 893–909

Ratté, J. C., and Gaskill, D. L., 1975, Reconnaissance geological map of the Gila Wilderness study area, southwestern New Mexico: U.S. Geological Survey, Miscellaneous Investigations Series, Map I-886

Ratté, J. C., Gaskill, D. L., Eaton, G. P., Peterson, D. L., Stotelmeyer, R. B., and Meeves, H. C., 1979, Mineral resources of the Gila Primitive area and Gila Wilderness, New Mexico: U.S. Geological Survey, Bull. 1451, p. 1-229

Reid, H. F., 1911, Remarkable earthquakes in central New Mexico in 1906 and 1907: Seismological Society of America, Bull., v. 1, p. 10–16

Richter, C. F., 1935, An instrumental earthquake magnitude scale: Seismological Society of America, Bull., v. 25, p. 1–32

Sinno, Y. A., Keller, G. R., and Sbar, M. L., 1981, A crustal seismic refraction study in west-central Arizona: Journal of Geophysical Research, v. 86, p. 5,023–5,038

U.S. Coast and Geodetic Survey, 1938, Abstracts of earthquake reports from the Pacific coast and the western mountain region: U.S. Department of Commerce, Seismological Field Survey, MSA-17 through MSA-20 (quarterly)

———, 1939, Abstracts of earthquake reports from the Pacific coast and the western mountain region: U.S. Department of Commerce, Seismological Field Survey, MSA-21 through MSA-24 (quarterly)

Warren, D. H., 1969, A seismic refraction survey of crustal structure in central Arizona: Geological Society of America, Bull., v. 80, p. 257–282 □

TABLE 2—MOGOLLON MOUNTAINS EARTHQUAKES OF 1938–39 (BASED ON TUO DATA, EPICENTERS AT 33.3°N., 108.5°W.).

Date yr mo day	Origin time (UTC)	$m_{b,int}$ Magnitude (eq 2)	(eq 3)	Total duration (seconds)	Maximum MM intensity	Date yr mo day	Origin time (UTC)	$m_{b,int}$ Magnitude (eq 2)	(eq 3)	Total duration (seconds)	Maximum MM intensity
1938 09 05	00 34 30	3.4		330		11 26	23 00 37	3.2		323	III
09 05	00 38 25	2.3		185		11 27	00 12 39	4.6		720	V
09 05	07 27 17		2.2	216		11 27	00 18 40	2.7		350	
09 06	09 14 06		1.9			11 27	00 23 39		1.4	180	
09 07	08 13 43		1.7			11 27	00 55 58		2.4	220	
09 17	17 20 17	4.9			VI	11 27	02 16 15		1.8	160	
09 17	18 29 54	2.6				11 27	04 03 20		2.2	215	
09 17	19 38 24	3.4			IV	11 27	08 14 35		2.0	180	
09 18	01 21 00	3.7				11 27	09 24 00		1.8	160	
09 18	01 48 54	2.6				11 27	12 16 06		1.9	165	
09 18	08 27 33		2.3			12 11	04 23 25		2.6	230	
09 18	10 21 48		2.0			12 18	01 07 35		1.9	210	
09 18	16 19 06	3.8		560		12 28	22 07 05	3.9			V
09 19	00 25 33	2.7		287	IV	1939 01 01	04 42 35		2.9	275	
09 19	10 42 59	3.7		400		01 02	13 15 28	2.6		275	
09 19	17 42 23		2.3	220		01 18	11 52 47	2.9		275	
09 19	21 57 31		1.3	150		01 18	13 57 11	2.6		245	IV
09 20	03 31 10		2.1	180		01 20	12 17 20	3.7		395	VI
09 20	04 22 59		2.0	186		01 29	23 50 20		2.9	245	
09 20	05 39 00	4.3		675	VI	02 03	15 57 51		3.4	295	
09 21	05 54 05	2.7		250		02 07	09 12 20		3.0	295	
09 21	17 09 04	2.6		305		02 12	01 56 37		2.7	223	
09 22	15 03 01		2.3	275		02 14	05 53 31		2.9	204	
09 22	20 12 31	3.0		275		02 18	04 13 36		3.3	364	
09 22	20 15 15	2.9		445		02 22	15 20 35	3.1		287	
09 23	03 01 11		2.1	225		02 24	12 02 02	3.4		403	
09 23	03 04 02		1.9	205		02 25	23 21 48		2.5	202	
09 23	03 59 41	3.1		320		03 06	23 10 34	3.0		361	
09 23	10 26 11	3.0		300		03 20	21 18 28	2.7		257	
09 24	00 23 37	2.7		303		03 24	12 11 44		2.5	248	
09 24	15 23 36	3.4		445	IV	03 24	19 21 55		2.5	270	
09 26	23 28 27		2.5	325		03 25	15 06 27	2.9		293	
09 29	23 31 44	4.3			V	04 08	09 42 24		2.5	222	
09 29	23 34 57	4.8		603	VI	04 25	17 16 50		1.9	185	III
09 29	23 44 15	3.3				04 26	01 57 06		2.0	174	III
09 30	00 46 11	2.9		364		05 22	00 16 39		2.8	216	IV
10 01	08 09 34		2.4	315		05 23	15 19 33		2.7	177	IV
10 01	08 32 53		2.1	195		06 04	01 19 10	4.6		590	VI
10 01	10 22 11		2.3	210		06 04	01 27 04	3.4		295	
10 01	13 14 38	3.6		447		06 04	09 08 00		2.8	255	
10 08	08 30 39	3.7		471		06 05	05 07 39	3.3		316	
10 10	03 35 27		2.8	295		06 07	06 02 16		2.5	224	
10 11	09 53 54		2.6	215		06 13	00 23 01		2.0	180	
10 16	13 03 46		2.1	230		07 01	20 32 23	4.0		600	
10 30	22 10 46	3.3		475	IV	07 01	20 36 41		3.0	339	
11 01	08 26 06	3.8		369	VI	07 02	13 08 01		2.7		
11 02	08 59 58	4.3		450	VI	07 11	19 54 05		2.0	165	
11 11	10 26 18	3.9		460	IV	07 17	06 58 25	3.7		415	
11 11	10 32 11		2.1	180		07 22	06 40 59		2.2		
11 22	18 11 43	2.6		220		07 29	00 24 05		2.7		IV